Int. J. Electrochem. Sci., 17 **(2022)** Article Number: 220119, doi: 10.20964/2022.01.09

International Journal of
ELECTROCHEMICAL
SCIENCE
www.electrochemsci.org

Preparation of electrochemical sensor based on β-cyclodextrin/Carbon Nanotube Nanocomposite for Donepezil Hydrochloride as drug for treatment of Alzheimer's Disease

Qiong Qin[1], *Xin Wang*[1], *Jincui Shi*[1], *Danfeng Wu*[2,*]

[1] Psychiatry Department, Wuhan Youfu Hospital, Wuhan, 430023, China
[2] Orthopaedics, Fifth Hospital in Wuhan, Wuhan, 430050, China
[*]E-mail: wdf3091@sina.com

Received: 5 September 2021 / *Accepted:* 27 October 2021 / *Published:* 6 December 2021

This study was conducted to prepare nanocomposite based carbon nanotubes (CNTs) and β-cyclodextrin-CNTs (βCD-CNTs) as an electrochemical sensor for determination of DNP as medicine for treatment of Alzheimer's disease. The electrodepositon method was used for modification of the glassy carbon electrode (GCE) surface with a nanocomposite of βCD-CNTs. The structural analyses of electrodeposited βCD-CNTs on the GCE surface using SEM and XRD revealed that βCD particles covered the high porous bundles of entangled CNTs surface and created of a highly cross-linked CNTs composite. The electrochemical characterizations using CV and DPV techniques showed the synergetic effect of CNTs and βCD molecules can improve the response of nanocomposite modified GCE to determine the DNP. Results showed that the response of βCD–CNTs/GCE was sensitive, selective and stable to determination of the DNP, and linear range, sensitivity, and limit of detection were obtained at 0 to 550 µM, 0.03233µA/µM and 8.5 nM, respectively. In prepared pharmaceutical samples of Aricept tablets, the precision and applicability of the βCD-CNTs/GCE for DNP determination sensor were evaluated, and the results showed that acceptable recovery (91.00 to 98.50%) and RSD (3.84 to 4.61%) values were obtained, as well as the appropriate performance of the βCD–CNTs/GCE for DNP determination sensor in clinical applications.

Keywords: CNTs; β-cyclodextrin; Nanocomposite; Electrodepositon; Donepezil hydrochloride; Differential pulse voltammetry

1. INTRODUCTION

Donepezil (DNP; 2-[(1-benzylpiperidin-4-yl)methyl]-5,6-dimethoxy-2,3-dihydroinden-1-one) is a piperidine derivative that has been shown to improve neurocognitive function. It is a new reversible inhibitor of the enzyme acetylcholinesterase (AChE) that breaks down the neurotransmitter acetylcholine [1, 2]. As a potent, selective and noncompetitive inhibitor of AChE through reversible

binding to AChE and inhibition of the hydrolysis of acetylcholine, as a consequences, it can increase the availability of acetylcholine at the synapses which leads to better communication between nerve cells and improved cholinergic function [3, 4]. Therefore, DNP has been used for the symptomatic treatment of mild to moderately severe Alzheimer's dementia [1, 5]. DNP may improve the ability to think and remember or slow the loss of these abilities in people who have Alzheimer's disease [6, 7]. However, donepezil will not cure Alzheimer's disease or prevent the loss of mental abilities at some time in the future [8, 9].

Like all medicines of Alzheimer's disease, DNP can cause side effects, although not everyone gets them [10]. The most common side effects of DNP are diarrhoea, headache, frequent urination, nausea, excessive tiredness and difficulty falling asleep or staying asleep [11]. In rare cases, it's possible to appearance a serious allergic reaction (anaphylaxis) to DNP [12].

Additionally, dosage and timing are important in medication administration of DNP. Therefore, determination of DNP content is necessary in pharmacology and taking medication. Accordingly, many studies have been performed for detecting of DNP concentration in clinical samples using high-performance liquid chromatography [13], mass spectrometry [14], ultraviolet absorbance detection [15] and electrochemistry [16-19]. Among these methods, electrochemical methods have been as economical and fast response for determination a wide range of chemical analytes. Moreover, studies based on the modification the electrodes in sensing systems have been indicated using the nanomaterials enhance sensitivity and selectivity [20, 21]. Thus, this work was conducted for preparation of nanocomposite based nanotube carbon and β-cyclodextrin as an electrochemical sensor for DNP.

2. MATERIALS AND METHOD

A homogeneous suspension of 0.5 mg/mL CNTs (Jiangsu Xfnano Materials Tech Co., Ltd., China) was prepared with deionized water, and 80 mg/mL of β-cyclodextrin (βCD, ≥97%, Sigma-Aldrich) aqueous solution was ultrasonically mixed the dispersed CNTs suspension in equal volume ratio [22]. Next, ammonia (28%, Shijiazhuang Chemical Tech Co., Ltd., China) and hydrazine (98%, Sigma-Aldrich) solutions was added the resulted suspension in volume ratio of 1:1:100. The resulted mixture was stirred for 10 minutes in room temperate, and subsequently transferred into a water bath at 55°C for 4 hours to obtain the stable black suspension. Then, the suspension was filtered with a polyester track etch membrane (PETE, 8μm, Sterlitech, USA). After then, the obtained βCD-CNTs nanocomposite were dispersed in 0.5 M PBS to obtain the mixture of 1.0 g/l of β-cyclodextrin-CNTs (βCD-CNTs) as electrolyte for electrodeposition of βCD-CNTs nanocomposite on GCE. Before the electrdeposition, the glassy carbon electrode (GCE) surface was polished with alumina slurries (1 and 0.3μm, 99%, Sigma-Aldrich) and rinsed with deionized water followed by washing with 0.05M nitric acid (69%, Merck, Germany), pure ethanol (95%, Shandong Aojin Chemical Technology Co., Ltd., China) and deionized water, respectively. The electrodeposition was performed using electrochemical workstation (CS150 professional potentiostat/galvanostat, Xian Yima Optoelec Co., Ltd., China) in three-electrode cell at potential range of -1.3 V to +0.7 V at scan rate of 10 mV/s for 12 minutes [23].

The electrochemical cell contained GCE s working electrode, Ag/AgCl (3M KCl) a reference, and a Pt plate as a counter electrode.

Aricept 5 mg tablets for oral administration were provided by a local pharmacy which contained 5 mg of donepezil hydrochloride. To prepare the initial DNP solution with a 0.01 mg/ml concentration as a pharmaceutical real sample, 2 tablets of Aricept were added to 100 ml of 0.1 M PBS under magnetic string at room temperature. The resultant mixture was centrifuged at 1500 rpm for 8 minutes, and the supernatant was stored at 4°C in the fridge for following electrochemical experiments.

Cyclic voltammetry (CV) and differential pulse voltammetry (DPV) experiments were conducted on the electrochemical workstation in 0.1M PBS pH 7.4 which was prepared from a mixture of Na_2HPO_4 (99.95%) and NaH_2PO_4 (≥99.0%, Sigma-Aldrich). For comparison of the obtained results, high performance liquid chromatography (HPLC, Tianjin Kermel Chemical Reagent Co. Ltd., China) was employed to determine DNP content in blood plasma. The morphology of prepared nanocomposite was studied using scanning electron microscopy (SEM, Jeol JSM 7500F, Japan). The crystal structure of nanostructures was analyzed using X-ray diffraction (XRD; 6000 X-radial, Shimadzu, Japan).

3. RESULTS AND DISCUSSION

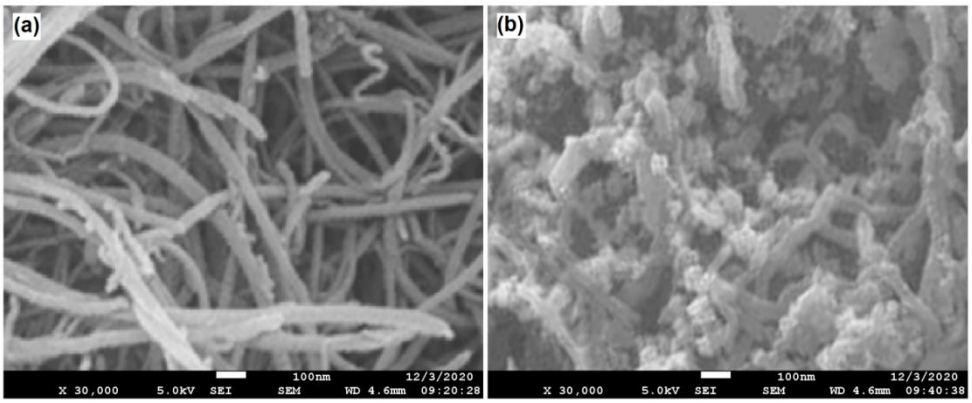

Figure 1. SEM images of (a) CNTs/GCE and (b) βCD-CNTs/GCE.

Figure 1 displays the FESEM image of CNTs/GCE and βCD-CNTs/GCE. As seen from Figure 1a, high density and high porosity bundles of entangled CNTs were electrodeposited on the surface of GCE which resulted in a low diffusion catalytic network and highly dense active sites for electrochemical reactions. The average diameter of CNTs is 70nm. Figure 1b shows the electrodeposited βCD–CNTs nanocomposite on the GCE surface, indicating the βCD particles cover the CNTs surface because of hydroxyl and amine groups on the βCD structure. The βCD particles can form π–π bonding interactions with CNTs and create a highly cross-linked CNTs composite [24].

Figure 2 reveals the results of XRD analysis of eletrodeposited powder of CNTs and βCD–CNTs on the GCE surface. It is observed from Fig. 2a, XRD patterns of CNTs show the two diffraction peaks at 2θ = 26.34° and 44.01°, which signify the (002) and (101) crystal planes of wall

carbon nanotubes, respectively [25], illustrating a highly ordered structure of CNTs. The XRD pattern of βCD–CNTs in Figure 2b not only shows (002) and (101) crystal planes of CNTs but also a broad diffraction peak at 2θ = 22.71° that is related to the disordered structure of βCD [26]. The decrease in diffraction peaks of CNTs can be attributed to the partial occupation of CNTs surfaces by βCD molecules [26].

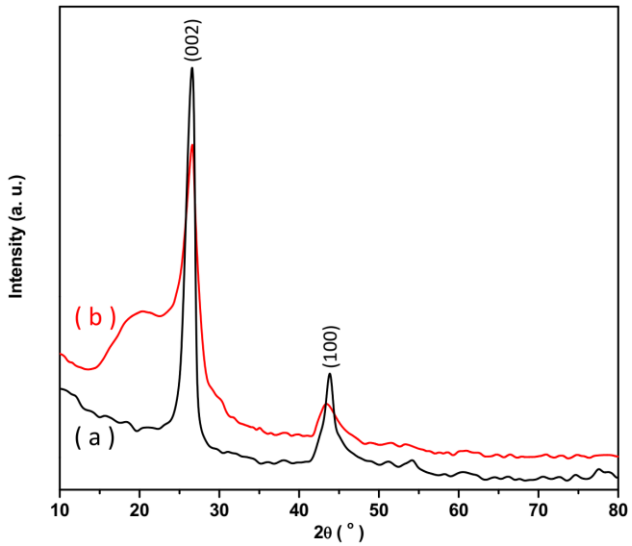

Figure 2. XRD pattern of electrodeposited powder of (a) CNTs and (b) βCD-CNTs on GCE surface

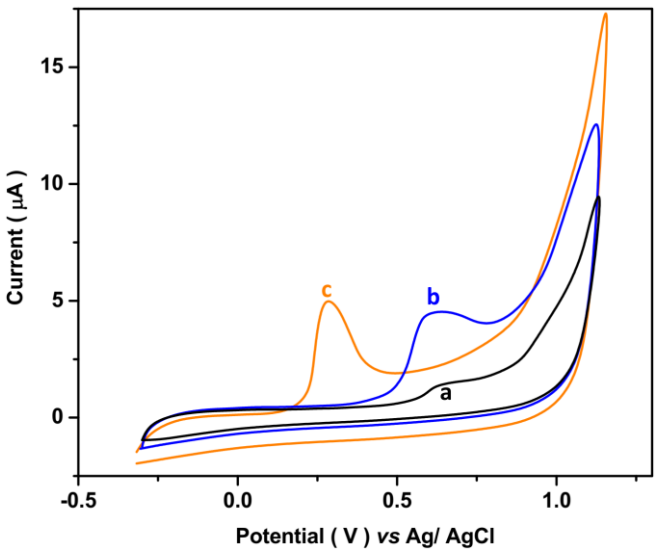

Figure 3. CV plots of (a) GCE, (d) CNTs/GCE and (c) βCD–CNTs/GCE in 0.1M PBS (pH=7.4) at a scanning rate of 20 mV/s in presence of 150 µM DNP solution.

Figure 3 shows the CV plots of GCE, CNTs/GCE and βCD-CNTs/GCE in 0.1M PBS (pH=7.4) at a scanning rate of 20mV/s in the presence of 150 µM DNP solution. As observed, CV plots of GCE, CNTs/GCE and βCD–CNT/GCE exhibit the anodic peaks at 0.7 V, 0.61 V and 0.29 V, respectively,

indicating irreversible oxidation of DNP as suggested in Figure 4 [16, 27]. It is found that peak potential is moved to less positive potentials by modification of the GCE with CNTs and βCD–CNTs. This can be attributed to a large edge plane/basal plane ratio of CNTs which can provide a larger real surface area and a high porous surface for fast electron transfer in electrochemical reactions [28, 29].

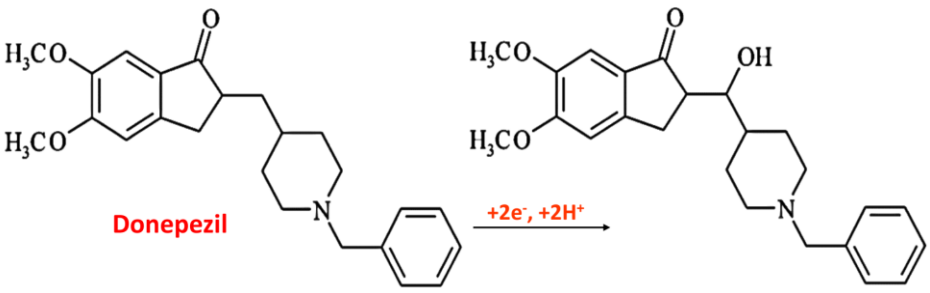

Figure 4. Suggesting mechanism for electrochemical oxidation of DNP [16].

The higher peak currents are observed for βCD–CNTs/GCE and CNTs/GCE because of CNTs's high electrical conductivity, excellent adsorptive ability and catalytic ability [30, 31].

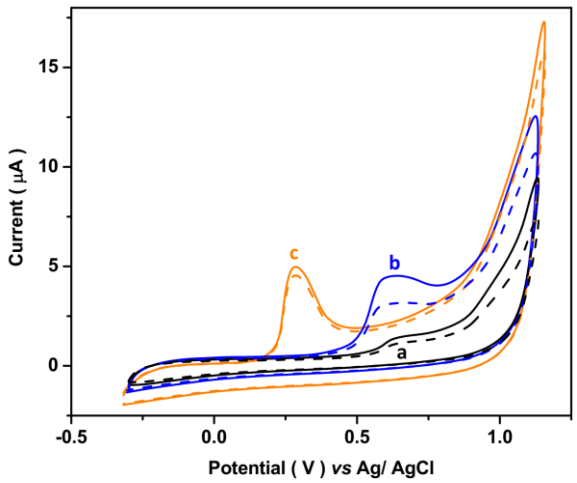

Figure 5. The first (solid line) and 50th (dashed line) CV responses of (a)GCE, (b)CNTs/GCE and (c) βCD–CNTs/GCE in 0.1 M PBS pH 7.4 at a scanning rate of 20 mV/s in presence of 150 μM DNP solution.

Moreover, comparison between the CNTs/GCE and βCD–CNTs/GCE reveals the significant βCDs particles effect on decreasing the oxidation potential and enhancement of peak current which can be related to the formation of an inclusion complex between cyclodextrin and the carbonyl group of DNP [32]. Therefore, the synergetic effect of CNTs and βCD molecules can improve the response of modified GCE and mass transferrin electrochemical reactions, which is attributed to the high surface area, superconductivity, disorder and defect structure of CNTs, and the supramolecular recognition

capability of βCD molecules to form inclusion complexes with many hydrophobic guest molecules such as DNP [33-35].

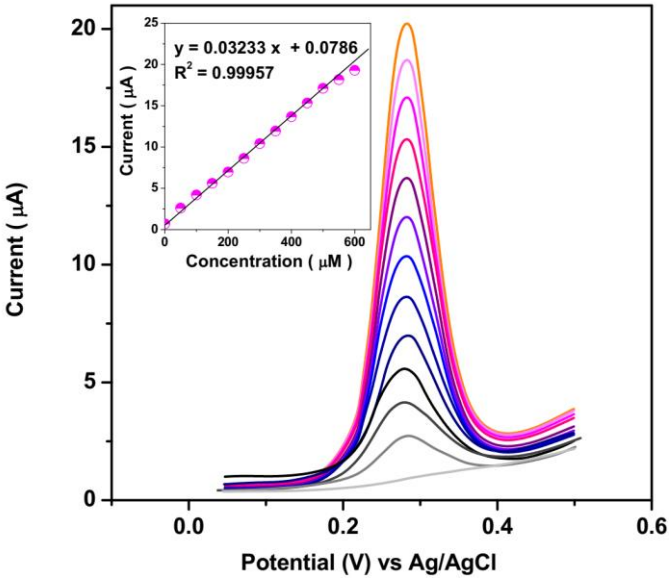

Figure 6. DPV response and obtained calibration graph of βCD–CNTs/GCE to add different DNP solution in 0.1 M PBS pH 7.4 at a scanning rate of 20mV/s.

Table 1. Comparison the performance of βCD–CNTs/GCE for electrochemical determination of DNP with other reported electrochemical DNP sensors.

Electrodes	**Method**	**Detection limit (nM)**	**Linear range (µM)**	**Ref.**
βCD–CNTs/GCE	DPV	8.5	0–550	This work
Gold Electrode	DPV	-	76.68- 172.33	[16]
βCD/carbon paste electrode	DPV	1.2	0.0032- 0.042	[17]
GCE	OSWV	263	1-100	[39]
Poly (solochrome black T)/N-doped carbon nanodots /Co NPs/pencil graphite electrode	CV	0.5	0.0015–400	[40]
Donepezil cation/polyvinylchloride membrane	Potentiometry	400	$1–10^{+4}$	[13]
Column with C_{18} precolumn inserts	HPLC-FD	2.23	0.006–5.27	[41]
Column with C_{18} Ace 5	HPLC	3689	65-330	[42]
Column with C_{30} Develosil Combi-RP5	HPLC	0.5	0.001–0.050	[43]
Column with C_{18} Phenyl Hypersil	HPLC	0.527	0.013–5.27	[44]

OSWV: Osteryoung square wave voltammetry; HPLC-FD: High-performance liquid chromatography with fluorescence detection.

The stability of the electrode response to DNP was investigated by recording successive CVs in an electrochemical cell. The first and 50th CV responses of GCE, CNTs/GCE, and βCD–CNTs/GCE in 0.1M PBS (pH=7.4) at a scanning rate of 20 mV/s in the presence of 150 M DNP solution are shown in Figure 5. Comparison between the first and 50^{th} CV response exhibits a 26%, 30%, and 9%

change in oxidation peak current of DNP on GCE, CNTs/GCE, and βCD–CNTs/GCE, respectively. Accordingly, the response of βCD–CNTs/GCE is more sensitive and stable than that of GCE and CNTs/GCE due to hydrophilic characteristics, high chemical mechanical stability, and the planar structure of CNTs leads to a larger effective surface area and more exposed active sites for the strong anchoring of the βCD molecules [33, 36-38]. Therefore, the βCD–CNTs/GCE was chosen for the following electrochemical study of DNP.

Figure 6 shows the DPV response and obtained calibration graph of βCD–CNTs/GCE to additions of different DNP solutions in 0.1M PBS (pH=7.4) at a scanning rate of 20 mV/s. It can be observed that the increase in DNP concentration in an electrochemical cell leads to a linear increase in DPV peak current from 0 to 550 µM. The obtained calibration graph indicates that the sensitivity and limit of detection of βCD–CNTs/GCE for determination of DNP are 0.03233µA/µM and 8.5 nM, respectively. Moreover, the performance of βCD-CNTs/GCE for electrochemical determination of DNP is compared with other reported electrochemical DNP sensors in Table 1. The comparison reveals that the linear range of βCD–CNTs/GCE is wider than other DNP sensors, and it can be associated with noncovalent/covalent functionalization of CNTs with βCD molecules [45]. βCD molecules can also form well-defined host-guest complexes with an analyte [33-35, 45]. As a consequence, βCD-CNTs/GCE shows enhanced electrochemical sensing performance for the electrochemical determination of DNP.

Table 2 shows the results of the investigation into the anti-interference capability and selectivity of βCD–CNTs/GCE for electrochemical determination of DNP through the DPV technique in 0.1M PBS (pH=7.4) at a scanning rate of 20 mV/s. Table 2 indicates that the of βCD–CNTs/GCE shows the significant response to addition 50 µM DNP on electrochemical cell, and 150 µM addition of co-administered medicines often taken with DNP, such as sertraline, mirtazapine, olanzapine, risperidone, ziprasidone, quetiapine, asenapine, gabapentin, pregabalin and piracetam do not interfere with the electrochemical determination of DNP. Therefore, the proposed sensor can be used as a DNP selective electrochemical sensor in pharmaceutical applications.

Table 2. Results of DPV responses of βCD–CNTs/GCE to addition 50 µM of DNP and 150 µM of interfering species in 0.1M PBS (pH=7.4) at a scanning rate of 20 mV/s.

Specie	Concentration (µM)	Electrocatalytic peak current at 0.29 V (µA)	RSD (%)
DNP	50	1.6159	±0.0115
Sertraline	150	0.0151	±0.0019
Mirtazapine	150	0.0227	±0.0011
Olanzapine	150	0.1063	±0.0030
Risperidone	150	0.0218	±0.0017
Ziprasidone	150	0.0815	±0.0015
Quetiapine	150	0.1188	±0.0020
Asenapine	150	0.1292	±0.0032
Gabapentin	150	0.2135	±0.0018
Pregabalin	150	0.3077	±0.0012
Piracetam	150	0.0870	±0.0017

RSD: Relative standard deviation

The precision and applicability of βCD–CNTs/GCE to the determination of DNP were evaluated in prepared pharmaceutical real samples. Figure 7 depicts the DPV curves and obtained calibration graph of βCD–CNTs/GCE in a prepared real sample of Aricept tablets with 0.1M PBS (pH=7.4) at a scanning rate of 20mV/s under successive additions of DNP solution. As observed from Figure 7, the DNP content in the produced sample is 0.009mg.ml^{-1}, which is near to the true value of the content of the DNP in a real sample of Aricept tablets (0.01 mg/ml). Furthermore, Table 3 shows the results of the analytical applicability of βCD–CNTs/GCE using the standard addition method, indicating the acceptable recovery (91.00 to 98.50%) and RSD (3.84 to 4.61 %) values, and verification of appropriate performance of βCD–CNTs/GCE to determine the DNP sensor in clinical applications.

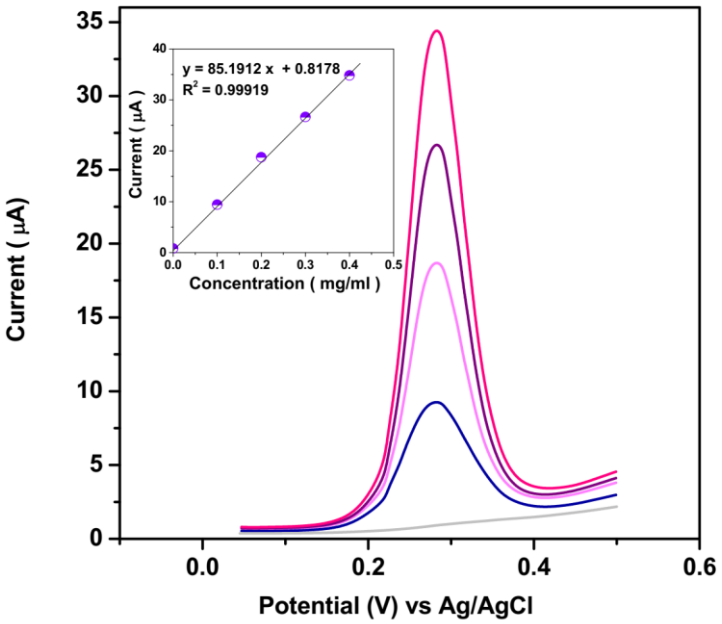

Figure 7. DPV curves and obtained calibration graph of βCD–CNTs/GCE in prepared real sample of Aricept tablets with 0.1M PBS (pH=7.4) at a scanning rate of 20mV/s under successive additions of DNP solution.

Table 3. Results of analytical applicability of βCD–CNTs/GCE to determine DNP in real samples of Aricept tablets

Added(mg/ml)	Found(mg/ml)	Recovery(%)	RSD(%)
0.100	0.091	91.00	3.84
0.200	0.186	93.00	3.95
0.300	0.290	96.66	4.24
0.400	0.394	98.50	4.61

Furthermore, the concentration of DNP in the plasma of five patients with Alzheimer's disease, aged 65 to 70 years, who had Aricept tablets treatment in Wuhan Mental Health Center (Wuhan, China), was determined roughly 5-6 hours after the dose. The blood plasma samples were centrifuged at 1000 rpm for 10 minutes and the resultant supernatants were utilized to prepare 0.1 M PBS (pH=7.4). Next, the βCD–CNTs/GCE was used to determine the concentration of DNP in the prepared real samples using the DPV technique. Table 4 presents the results of an average of six determinations of DNP for each sample using the βCD–CNTs/GCE and HPLC techniques, respectively. The result reveals good agreement between the βCD–CNTs/GCE sensor and HPLC techniques, and RSD (2.61% to 4.33%) values demonstrating high precision between the two techniques.

Table 4. Results of determinations of DNP content in prepared real samples of blood plasma of five patients aged 65 to 70 years with Alzheimer's disease who underwent Aricept tablets treatment through the βCD–CNTs/GCE sensor and HPLC technique.

Sample No.	Content of DNP in prepared real plasma sample (nM)			
	βCD–CNTs/GCE	RSD (%)	HPLC	RSD (%)
1	9.032	±3.11	8.992	±4.12
2	9.240	±3.77	9.457	±3.13
3	8.588	±2.61	8.601	±3.85
4	9.923	±4.33	10.071	±2.71
5	8.735	±3.81	8.828	±3.95

4. CONCULUSION

This study was presented the preparation of βCD-CNTs nanocomposite and electrodepositing on the GCE surface, and the study of its application as an electrochemical sensor for the determination of DNP. The structural analyses of the electrodeposited βCD-CNTs nanocomposite on the GCE surface exhibited that βCD particles covered the high porosity bundles of entangled CNTs surface and created of a highly cross-linked CNTs composite. The electrochemical characterizations showed that the response of βCD–CNTs/GCE was sensitive, selective and stable to determination of the DNP, and linear range, sensitivity and limit of detection were obtained at 0 to 550 μM, 0.03233μA/μM and 8.5nM, respectively. The results of the study on the precision and applicability of βCD–CNTs/GCE for determination of DNP in prepared pharmaceutical samples of Aricept tablets revealed the acceptable recovery and RSD values, and indicated the appropriate performance of βCD–CNTs/GCE for the determination of DNP sensors in clinical applications.

References

1. H. Sugimoto, H. Ogura, Y. Arai, Y. Iimura and Y. Yamanishi, *The Japanese journal of pharmacology*, 89 (2002) 7.

2. Y. Orooji, P.N. Asrami, H. Beitollahi, S. Tajik, M. Alizadeh, S. Salmanpour, M. Baghayeri, J. Rouhi, A.L. Sanati and F. Karimi, *Journal of Food Measurement and Characterization*, (2021) 1.
3. H. Karimi-Maleh, Y. Orooji, F. Karimi, M. Alizadeh, M. Baghayeri, J. Rouhi, S. Tajik, H. Beitollahi, S. Agarwal and V.K. Gupta, *Biosensors and Bioelectronics*, 184 (2021) 113252.
4. J. Yan, Y. Meng, X. Yang, X. Luo and X. Guan, *IEEE Transactions on Information Forensics and Security*, 16 (2020) 1880.
5. E.L. Barner and S.L. Gray, *Annals of Pharmacotherapy*, 32 (1998) 70.
6. H. Karimi-Maleh, M.L. Yola, N. Atar, Y. Orooji, F. Karimi, P.S. Kumar, J. Rouhi and M. Baghayeri, *Journal of colloid and interface science*, 592 (2021) 174.
7. B. Zhou, Z. Liu, C. Li, M. Liu, L. Jiang, Y. Zhou, F.L. Zhou, S. Chen, S. Jerrams and J. Yu, *Advanced Electronic Materials*, 7 (2021) 2100233.
8. B. Jiang, Y. Liu, L. Zhao, L. Zhao, C. Wang, C. Liu and B. Xu, *Soft Matter*, 17 (2021) 7516.
9. L.-B. Hu, X.-Y. Huang, S. Zhang, X. Chen, X.-H. Dong, H. Jin, Z.-Y. Jiang, X.-R. Gong, Y.-X. Xie and C. Li, *Journal of materials science. Materials in electronics*, 32 (2021) 23728.
10. X. Ji, C. Hou, M. Shi, Y. Yan and Y. Liu, *Food Reviews International*, (2020) 1.
11. N. Dunn, G. Pearce and S. Shakir, *Journal of Psychopharmacology*, 14 (2000) 406.
12. C. Hou, M. Yin, P. Lan, H. Wang, H. Nie and X. Ji, *Chemical and Biological Technologies in Agriculture*, 8 (2021) 1.
13. G.A.H. Mostafa, M. Hefnawy and A. Al-Majed, *Journal of AOAC International*, 93 (2010) 549.
14. K. Matsui, Y. Oda, H. Nakata and T. Yoshimura, *Journal of Chromatography B: Biomedical Sciences and Applications*, 729 (1999) 147.
15. N. Yasui-Furukori, R. Furuya, T. Takahata and T. Tateishi, *Journal of Chromatography B*, 768 (2002) 261.
16. A.R. Mladenović, D.Ž. Mijin, S.Ž. Drmanić, V.E. Vajs, V.M. Jovanović, S.D. Petrović and M.L.A. Ivić, *Electroanalysis*, 26 (2014) 893.
17. C. Rao, K. Subbarayudu and P. Venkateswarlu, *Portugaliae Electrochimica Acta*, 28 (2010) 349.
18. A. Gencturk and A.S. Sarac, *International Journal of Electrochemical Science*, 11 (2016) 111.
19. Y. Orooji, B. Tanhaei, A. Ayati, S.H. Tabrizi, M. Alizadeh, F.F. Bamoharram, F. Karimi, S. Salmanpour, J. Rouhi and S. Afshar, *Chemosphere*, 281 (2021) 130795.
20. Z. Savari, S. Soltanian, A. Noorbakhsh, A. Salimi, M. Najafi and P. Servati, *Sensors and Actuators B: Chemical*, 176 (2013) 335.
21. H. Savaloni, E. Khani, R. Savari, F. Chahshouri and F. Placido, *Applied Physics A*, 127 (2021) 1.
22. Y. Guo, S. Guo, J. Ren, Y. Zhai, S. Dong and E. Wang, *ACS nano*, 4 (2010)
23. L. Chen, Y. Tang, K. Wang, C. Liu and S. Luo, *Electrochemistry communications*, 13 (2011) 133.
24. N. Farhadian, A. Sharifi and E. Lashgari, *Biomedical Chromatography*, 29 (2015) 366.
25. D.K. Singh, P. Iyer and P. Giri, *Diamond and Related Materials*, 19 (2010) 1281.
26. C. Liu, H. Zhao, P. Hou, B. Qian, X. Wang, C. Guo and L. Wang, *ACS applied materials & interfaces*, 10 (2018) 36229.
27. N.K. Ramadan, A.R. Derar, T.A. Mohamed, M.A. Sliem and A.A. Moustafa, *Analytical & Bioanalytical Electrochemistry*, 10 (2018) 1259.
28. M. Zhou and S. Guo, *ChemCatChem*, 7 (2015) 2744.
29. R. Savari, J. Rouhi, O. Fakhar, S. Kakooei, D. Pourzadeh, O. Jahanbakhsh and S. Shojaei, *Ceramics International*, 47 (2021) 31927.
30. S.-J. Young, Z.-D. Lin, C.-H. Hsiao and C.-S. Huang, *International Journal of Electrochemical Science*, 7 (2012) 11634.

31. W. Guo, M. Geng, L. Zhou, S. Chao, R. Yang, H. An, H. Liu and C. Cui, *International Journal of Electrochemical Science*, 8 (2013) 5369.
32. I. Bratu, F. Veiga, C. Fernandes, A. Hernanz and J. Gavira, *Spectroscopy*, 18 (2004) 459.
33. Y. Zhao, X. Zheng, Q. Wang, T. Zhe, Y. Bai, T. Bu, M. Zhang and L. Wang, *Food Chemistry*, 333 (2020) 127495.
34. B. Mirzaei, A. Zarrabi, A. Noorbakhsh, A. Amini and P. Makvandi, *RSC Advances*, 11 (2021) 7862.
35. P. Sozio, L.S. Cerasa, L. Marinelli and A. Di Stefano, *Neuropsychiatric disease and treatment*, 8 (2012) 361.
36. R. Savari, H. Savaloni, S. Abbasi and F. Placido, *Sensors and Actuators B: Chemical*, 266 (2018) 620.
37. H. Savaloni, R. Savari and S. Abbasi, *Current Applied Physics*, 18 (2018) 869.
38. F. Chahshouri, H. Savaloni, E. Khani and R. Savari, *Journal of Micromechanics and Microengineering*, 30 (2020) 075001.
39. A. Golcu and S. Ozkan, *Die Pharmazie-An International Journal of Pharmaceutical Sciences*, 61 (2006) 760.
40. F.A. Mohamed, P.Y. Khashaba, R.Y. Shahin and M.M. El-Wekil, *Colloids and Surfaces A: Physicochemical and Engineering Aspects*, 567 (2019) 76.
41. F.A. Mohamed, P.Y. Khashaba, R.Y. Shahin and M.M. El-Wekil, *Royal Society open science*, 6 (2019) 181476.
42. İ. Bulduk and B.S. Aydın, *Journal of Chemical Metrology*, 14 (2020) 1.
43. K. Nakashima, K. Itoh, M. Kono, M.N. Nakashima and M. Wada, *Journal of pharmaceutical and biomedical analysis*, 41 (2006) 201.
44. M. Abonassif, M. Hefnawy, M. Kassem and G. Mostafa, *Acta Pharmaceutica*, 61 (2011) 403.
45. A.U. Alam and M.J. Deen, *Analytical Chemistry*, 92 (2020) 5532.